The LDL Receptor Clustering Motif Interacts with the Clathrin Terminal Domain in a Reverse Turn Conformation

Richard G. Kibbey,* Josep Rizo,‡§ Lila M. Gierasch,‖ and Richard G.W. Anderson*

*Department of Cell Biology and Neuroscience, ‡Department of Biochemistry, and §Department of Pharmacology, University of Texas Southwestern Medical Center, Dallas, Texas, 75235; and ‖Department of Chemistry, University of Massachusetts, Amherst, Massachusetts 01003

Abstract. Previously the hexapeptide motif $FXNPXY_{807}$ in the cytoplasmic tail of the LDL receptor was shown to be essential for clustering in clathrin-coated pits. We used nuclear magnetic resonance line-broadening and transferred nuclear Overhauser effect measurements to identify the molecule in the clathrin lattice that interacts with this hexapeptide, and determined the structure of the bound motif. The wild-type peptide bound in a single conformation with a reverse turn at residues NPVY. $Tyr_{807}Ser$, a peptide that harbors a mutation that disrupts receptor clustering, displayed markedly reduced interactions. Clustering motif peptides interacted with clathrin cages assembled in the presence or absence of AP2, with recombinant clathrin terminal domains, but not with clathrin hubs. The identification of terminal domains as the primary site of interaction for $FXNPXY_{807}$ suggests that adaptor molecules are not required for receptor-mediated endocytosis of LDL, and that at least two different tyrosine-based internalization motifs exist for clustering receptors in coated pits.

Key words: clathrin • endocytosis • LDL receptor • nuclear magnetic resonance

RECEPTOR-MEDIATED endocytosis via clathrin-coated pits is a major mechanism by which cells internalize extracellular ligands and regulate cell surface receptor traffic. The internalization-defective LDL receptor was the first example of a protein bearing a mutation that prevents sorting during endocytosis (1). A conserved hexapeptide sequence in the cytoplasmic tail of the LDL receptor (FXNPXY where X is any amino acid) has since been found to be necessary and sufficient for coated pit clustering (9, 13, 14). This sequence has been predicted to form a reverse turn conformation (12), and the presence of this conformation in peptides corresponding to the cytoplasmic portion of a receptor strongly correlates with the efficiency of internalization in cultured fibroblasts (2). The signal for targeting a membrane protein to coated pits, therefore, depends upon the secondary structure of the FXNPXY motif.

In contrast to the clear identification of a motif responsible for LDL receptor clustering, the identity of the molecule(s) within coated pits responsible for capturing the LDL receptor is not known. Candidate molecules include the clathrin triskelion and AP2, the two structural components of the lattice. Each triskelion is composed of three heavy (~180 kD) and three light (~33 kD) chain molecules. AP2, by contrast, consists of four subunits: two of ~100 kD (adaptins), one of ~50 kD (designated the μ chain), and one of ~20 kD. The carboxy terminus of three clathrin heavy chains are linked together to form the hub of the triskelion, while the amino terminus of each has a flexible globular domain (~55 kD). When the triskelions are assembled into a lattice, the globular domain protrudes inwardly towards the membrane, and is able to extend and retract over a range of 15–20 nm (21). This domain as well as the hub is thought to bind APs (23, 24, 34) that are bound to the membrane by a high-affinity binding site (30, 58). Therefore, the globular domains of each triskelion in an assembled lattice are in close proximity to the plane of the membrane.

Originally, receptor clustering in coated pits was thought to involve a simple interaction between a tyrosine-based motif in the cytoplasmic portion of the receptor and one or more components of the clathrin lattice (41). The candidate interacting units were an NPXY motif in the receptors (9) and AP2 in the lattice (42). The model became more complex with the discovery of two additional internalization motifs: YXXΦ (where Φ is large hydrophobic) and dileucine (reviewed in 50). Additionally, β-arrestin acts as an adaptor molecule that targets phosphorylated

β_2-adrenergic receptors to coated pits (18). Clathrin appears to be the molecule in coated pits that captures arrestin, while the μ chain of AP2 may be responsible for clustering receptors containing YXXΦ motifs (4, 38, 39). Recently, dileucine motifs have been shown to interact with the β subunit of AP-1 (43). Receptors like the EGF receptor contain both YXXΦ and NPXY motifs, though it is unclear how the motifs function in endocytosis. For instance, the EGF receptor coimmunoprecipitates with AP2 after ligand binding (47), but mutations within the tail of the EGF receptor that prevent interactions with AP2 do not affect receptor internalization (35). Moreover, AP2 binding has been mapped to a region that contains a YXXΦ motif, but the EGF receptor does not compete for internalization with transferrin receptor, which also has a YXXΦ motif (56). Receptors with YXXΦ or dileucine motifs also do not compete with each other for internalization (31). The cytoplasmic tails of receptors, therefore, can contain multiple overlapping signals for targeting to coated pits and to other membrane domains (7, 32, 45, 50).

Attempts to detect interactions between AP2 and the FXNPXY motif using plasmon resonance have failed, and a combinatorial library showed no preference for FXN-PXY (4). Clustering of the LDL receptor may be due to weak protein–protein interactions depending on the cooperative behavior of multiple proteins in the lattice, or may require a novel adaptor molecule. The methods used so far have not identified interactions between the FXNPXY motif and any of these molecules. Another approach is to use nuclear magnetic resonance (NMR)[1] spectroscopy to detect interactions between internalization peptides and clathrin cages. NMR parameters such as line widths (defined as the peak width at half height) and nuclear Overhauser effect (NOE) buildup rates change when a rapidly tumbling peptide binds to a slowly rotating macromolecule or molecular complex. These changes identify specific interactions, and provide three-dimensional information about the bound conformation of the peptide. A major advantage of this technique is the ability to test for interactions between the peptide and a macromolecular system (26). Using this approach, we have identified the globular domain of the clathrin triskelion as a principle site of interaction during LDL receptor clustering in coated pits.

Materials and Methods

Peptide Synthesis

The peptides FDNPVYQKTT, FDNPVY, FDNPVSQKTT, FDNPVS, FDNPVA, FDNPVF, and FDNPVL were synthesized using standard FMOC chemistry with a free COOH terminus and an acylated NH_2 terminus. Crude peptides were purified by reverse-phase HPLC on a C18 column (Vydac, Hesperia, CA), equilibrated in H_2O with 0.1% trifluoroacetic acid, and eluted with a linear gradient of acetonitrile. The identities of the peptides were confirmed by mass spectrometry and amino acid analysis. Concentrated stock solutions of peptides were made by dissolving the peptide in D_2O and adjusting the pH to 6.0 with aliquots of concentrated NaOH.

---

1. *Abbreviations used in this paper*: GST, glutathione-S-transferase; m, medium; NMR, nuclear magnetic resonance; NOE, nuclear Overhauser effect; PTB, phosphotyrosine binding; s, strong; w, weak.

Purification and Assembly of Clathrin/AP Cages

Clathrin coat proteins were isolated from bovine brain by standard procedures (8). The coat proteins were then gel-filtered over a Superdex 200 column (Pharmacia Biotech, Inc., Piscataway, NJ) equilibrated in 0.6 M Tris at pH 9.0. Clathrin and AP fractions were pooled and loaded directly onto an anion exchange column (Source Q 15; Pharmacia Biotech, Inc.) equilibrated in 20 mM ethanolamine, pH 9.0, and eluted with a steep linear gradient of 1 M NaBr. Clathrin and AP fractions were pooled and concentrated using Centriprep 30 (Amicon Corp., Easton, TX). Concentrated proteins were polymerized (25) by extensive dialysis against NMR sample buffer (40 mM D_4-malonic acid [Cambridge Isotope Labs, Andover, MA], pH 6.0, 0.2 mM EDTA, 0.2 mM DTT, and 3 mM NaN_3). Protein concentration of the polymerized cage complex was determined using the Bradford reagent (Bio-Rad Laboratories, Hercules, CA).

For preparation of cages composed of clathrin or clathrin and AP2, the purification was slightly modified. An additional anion exchange chromatography step was performed to separate clathrin from AP2 before gel filtration. Each protein was then purified separately as before. AP-2 containing fractions from the second anion exchange step were then pooled on the basis of Coomassie blue–stained SDS-PAGE. The clathrin fraction was divided in half, and all of the AP-2 sample was added to one half of the clathrin. Both samples were concentrated in Centriprep 30 and dialyzed extensively as described above. Equal total protein amounts of clathrin or clathrin/AP-2 cages were added to each NMR sample, which contained clathrin (9.7 mg/ml) or clathrin (8.5 mg/ml) and AP-2 (1.2 mg/ml). Sample purity was confirmed by Coomassie blue–stained SDS-PAGE gels and by Western blotting with an antibody against β-adaptin (100/1; Sigma Chemical Co., St. Louis, MO).

Expression and Purification of Recombinant Proteins

The clathrin terminal domain (residues 1–579) was expressed as a glutathione-S-transferase (GST) fusion protein in *Escherichia coli* BL21 cells, and was prepared as described (17). Glutathione agarose beads (Sigma Chemical Co.) with the bound GST construct were then washed with thrombin cleavage buffer (50 mM Tris, 2.5 mM $CaCl_2$, 150 mM NaCl, pH 7.4). The beads were incubated overnight with gentle agitation in the presence of thrombin (Sigma Chemcial Co.). DTT was added to 10 mM and allowed to incubate an additional 1 h before eluting the cleaved terminal domain construct from the beads. Samples were concentrated and dialyzed overnight against NMR sample buffer with 100 mM KCl.

The clathrin hub construct (residues 1074–1483) was expressed as a hexahistidine construct in *E. coli* BL21(DE) cells as described (29). Bacterial lysates were incubated with Ni-NTA agarose (QIAGEN Inc., Valencia, CA) overnight and eluted with 250 mM imidazole in 50 mM Tris, pH 7.8. The eluted polypeptides were then loaded directly onto an anion exchange column equilibrated in 30 mM Tris, 1 mM EDTA, pH 7.8, and eluted with a linear gradient of 0.5 M KCl. Fractions were pooled on the basis of Coomassie blue–stained SDS-PAGE gels. Because the hub polypeptide aggregated in the NMR sample buffer, both the terminal domain and hub polypeptides were dialyzed against 40 mM KPO_4, 150 mM KCl, 0.2 mM EDTA, 3 mM NaN_3, and 0.2 mM DTT pH 7.2.

NMR Spectroscopy

All spectra were acquired at 500 MHz and 25°C in sample buffer containing 10% D_2O on a Varian Unity 500 spectrometer with a 5999.7-Hz spectral width using 3-(tetramethylsilyl) propionic acid as a chemical shift reference. 1D spectra were acquired with 128 transients of 64,000 points zero filled to 131,072 points (see Fig. 1) or 64 transients of 32,000 points zero filled to 65,536 points (see Figs. 4 and 5). Line-broadening was measured as the difference of peak widths at half height using the Felix 2.30 (Biosym Technologies) program. The broadening is reported as the line-width of the resonance peak in the presence of cages minus the line-width in the absence of cages. Crosspeak intensities were calculated in arbitrary units of volume using the Felix 2.30 program from spectra acquired at 60-, 100-, 140-, and 220-ms mixing times. The spectra were acquired in phase-sensitive mode (48) with 2×256 FIDs of 1024 complex points each. A spectral width of 5999.7 Hz was used in both dimensions, and 32 transients per FID were collected. The water signal was suppressed by presaturation.

The relative K_d for wild-type and position 807 mutant peptides from clathrin terminal domains was obtained from measurements of the peak intensities of the Phe (3, 5) aromatic protons for each of the peptides in the presence and absence of protein. The free and bound populations were calculated from the following equation:

$$\frac{1}{i_o} = \frac{p^f}{i_f} + \frac{p^b}{i_b}$$

where i is the intensity of the free (i_f), the bound (i_b), and observed (i_o) resonance, and p^f and p^b are the free and bound populations, respectively. Since peak intensities are inversely proportional to the transverse relaxation rate ($1/T_2$), the population of the free and bound peptide can be estimated from the change in intensity of a given peptide resonance upon addition of clathrin terminal domain if the T_2 of the resonance in the free and bound forms is known. The T_2 for a protein is approximately proportional to the molecular weight, and from the line-widths observed in 20-kD proteins (3), the expected T_2 for a 55-kD protein is ~10 ms. The T_2 calculated from the line-widths of several resonances of the free peptides was ~100 ms. The values of i_b were estimated to be $i_f/10$, assuming that the T_2s of the free and bound resonances are 100 and 10 ms, respectively. Therefore, the calculated populations of p^f and p^b were then used to obtain K_ds assuming standard protein–ligand equilibrium. Since the K_ds were based on T_2 estimates, their absolute values are likely to be inaccurate. However, the relative values of the K_ds can be compared because they were all obtained by the same method.

Distances were calculated only for interresidue NOEs seen in 60 ms mixing time data sets. Sequential Hα to NH NOEs were not used because they contained contributions from the free peptide. NOE distance restraints were calculated from both wild-type hexa- and decapeptide either by using bins of weak (w; 1.8–2.3 Å), medium (m; 1.8–3.5 Å), and strong (s; 1.8–5.0 Å) peaks, or by measured NOE volumes calibrated individually for each dimension with the average volume of the Phe, Tyr, and Pro (β/β) NOEs corresponding to 1.75 Å. Structures were calculated by simulated annealing performed with the programs INSIGHTII and NMRCHITECT (Biosym Technologies, San Diego, CA) incorporating either type of restraint. In short, peptides were heated to 1,000 K, and then the distance and chiral restraints were slowly increased over 30 ps. The peptides were then slowly cooled to 300 K while increasing covalent and nonbond forces over 32 ps. The final structures were then obtained by iteratively minimizing to a final derivative of 0.01 kcal/mol^{-1}/Å^{-2} and simulating 30 ps of restrained dynamics. Similar sets of structures were obtained with both sets of restraints. Stereospecific assignments of Pro(β,d,γ) were based on interresidue distances and geometry. Removal of pseudoatom restraints for Tyr (δ, ε) and Phe(δ) was based on the geometry of an initial set of structures. The final set of 30 restraints was (* denotes pseudoatom and distance is denoted as s, m, or w): Ac(Me*)::F(Hδ₁), w; F(Hδ₁):: D(HN), w; F(Hβ₂)::D(HN), w; D(Hβ₂)::N(HN), w; N(Hβ₁)::P(Hδ₅), w; N(Hβ₂)::P(Hδ₅), m; N(Hβ₁)::P(Hδ_R), w; N(Hβ₂)::P(Hδ_R), w; N(HN):: P(Hδ_R), w; P(Hβ_R)::V(HN), m; P(Hβ₅)::V(HN), w; P(Hδ₅)::V(HN), w; V(HN)::Y(HN), s; V(HN)::Y(Hδ₁), w; V(Hγ₁*)::Y(Hδ₁), w; V(Hγ₁*):: Y(Hε₁), w; Ac(Me*)::D(HN), w; Ac(Me*)::N(Hδ₂₁), w; Ac(Me*):: N(Hδ₂₂), w; V(HN)::N(Hβ₁), w; V(HN)::N(Hβ₂), w; N(Hβ₁)::Y(Hδ₂), w; N(Hβ₂)::Y(Hδ₁), w; P(Hγ₅)::Y(Hδ₁), w; P(Hγ₅)::Y(Hε₁), w; P(Hγ₅):: Y(HN), m; P(Hβ_r)::Y(HN), w; P(Hβ_r)::Y(Hδ₁), w; P(Hβ_r)::Y(Hε₁), w; P(Hα)::Y(HN), w.

Results

Clathrin triskelions and APs purified from bovine brain were assembled into membrane-free polyhedral cages using standard methods (25). We prepared synthetic hexa- and decapeptides corresponding to the wild-type LDL receptor internalization motif (FDNPVY and FDNPVYQKTT) and to an internalization defective motif (FDNPV**S** and FDNPV**S**QKTT). Aromatic (Fig. 1, *A–F*) and aliphatic (Fig. 1, *G* and *H*) side chain regions from one-dimensional ^{1}H NMR spectra are shown for peptide samples (2.5 mM) mixed with NMR sample buffer alone, or buffer containing clathrin cages (20 mg/ml). The wild-type and mutant peptides exhibited characteristic narrow ^{1}H line-widths in the absence of cages (Fig. 1, *A*, *D*, and *G*, and data not shown). Adding cages to wild-type hexa- and decapeptides caused a pronounced increase in the line widths, indicative of an interaction between the peptide and the cages and a consequent slower effective tumbling time for the peptide (Fig. 1, *B*, *C*, and *H*; 36). By contrast,

the cage-induced line-broadening of mutant peptides was markedly less than that of wild-type for both the hexa- and decapeptides, indicating a weaker interaction (Fig. 1, *E* and *F*). As a control for nonspecific binding or viscosity-induced broadening, we examined the decapeptides in the presence of 20 mg/ml BSA. Neither peptide displayed appreciable line-broadening (data not shown).

NOE spectroscopy (NOESY) is another method of detecting interactions between peptides and large protein complexes (26). The hexa- and decapeptides have inefficient cross-relaxation due to their small size, and thus have NOE spectra relatively devoid of cross-peaks (data not shown). A peptide interacting with a large protein complex will develop stronger NOEs because cross-relaxation is more efficient in the bound state. The resulting spin populations are then maintained in the free state where they are observed as an increase in the number and intensity of NOE crosspeaks (10, 11). As shown in Fig. 2 (*A* and *C*), the NOESY spectra of both the deca- and the hexa-wild-type peptides in the presence of cages contain numerous cross-peaks, many of which are strong. In contrast, only a few cross-peaks are observed in the NOESY spectra of the mutant peptides in the presence of cages (Fig. 2, *B* and *D*). The large difference in number and intensity of NOEs at a short mixing time (60 ms) is consistent with the line-broadening results (Fig. 1), and indicates that the wild-type peptides have higher affinity for the cages. Transferred NOEs were not observed with either wild-type or mutant decapeptide in solutions with 20 mg/ml BSA, even at long mixing times (300 ms; data not shown).
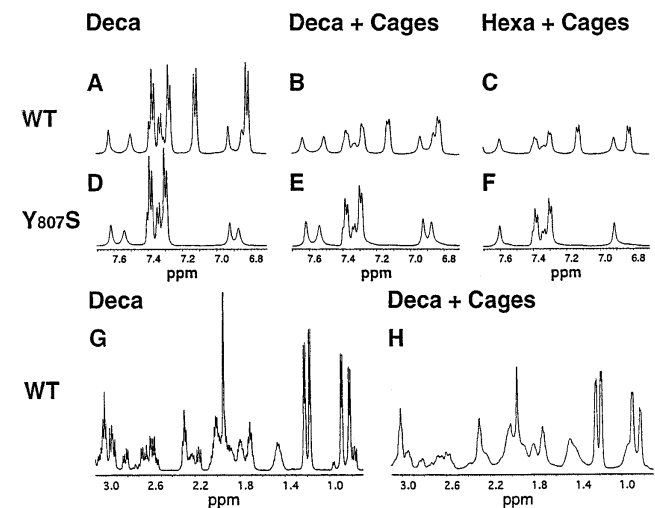

Figure 1. Differential line-broadening of internalization peptides in the presence and absence of clathrin-AP cages. Corresponding regions of 1-dimensional ^{1}H NMR spectra are shown at absolute intensity for 2.5 mM peptide with or without 20 mg/ml assembled clathrin/AP cages. (*A–F*) Aromatic region of the spectrum from wild-type peptides FDNPVYQKTT alone (*A*), FDNPVYQKTT plus cages (*B*), FDNPVY plus cages (*C*), and Y₈₀₇S mutant peptides FDNPVSQKTT alone (*D*), FDNPVSQKTT plus cages (*E*), and FDNPVS plus cages (*F*). (*G* and *H*) Upfield region of wild-type peptide, FDNPVYQKTT, alone (*G*) and with cages (*H*). The resonances of the aromatic protons are at 7.29, 7.33, and 7.38 ppm for Phe and 6.81 and 7.12 ppm for Tyr and for the methyl protons at 0.83 and 0.89 ppm for Val(γ), 1.25 ppm for Thr₉(γ), and 1.18 ppm for Thr₁₀(γ).

FDNPVY (A) FDNPVS (B)
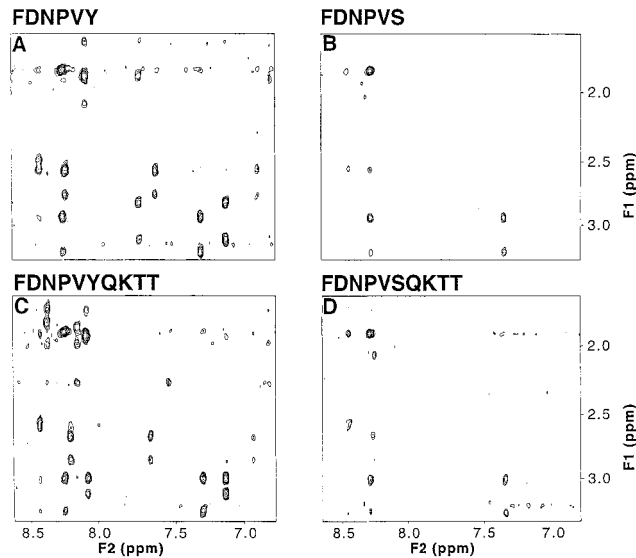
FDNPVYQKTT (C) FDNPVSQKTT (D)

Figure 2. NOESY spectra of wild-type and mutant internalization motif peptides in the presence of clathrin-AP cages. Samples were the same as those in the spectra of Fig. 1. Corresponding expansions from the aliphatic/amide + aromatic region of NOESY spectra are presented as contour plots at the same level from data acquired with 60 ms of mixing time. All samples contained 20 mg/ml cages and 2.5 mM peptide: FDNPVY (*A*), FDNPVS (*B*), FDN-PVYQKTT (*C*), and FDNPVSQKTT (*D*).

When a peptide binds to a macromolecule, the effective tumbling rates are slower for protons in the region of the peptide involved in binding, since protons in other regions are likely to experience fast internal motions. Thus, cross-relaxation is more efficient in the regions immobilized by binding, resulting in faster NOE buildup rates for a given fixed distance. To analyze the mobility of residues of the wild-type decapeptide bound to the cages, we first compared the build-up rates of transferred NOEs corresponding to covalently fixed equivalent proton distances. The similarity in NOE buildup rates (measured with 60-, 100-, 140-, and 220-ms mixing times) for the geminal β protons from residues F, N, P, and Y indicates that these residues behave isotropically in the bound state (Fig. 3 *A*). This phenomenon was also apparent in the similar line-broadening of the Tyr (εH, 3.45 Hz) and Phe (εH, 3.60 Hz) ring protons (Fig. 1). By contrast, the buildup rates for Hβ/Hγ NOEs decrease towards the COOH terminus of the peptide. Val has the most rapid buildup rate, indicating that it is immobilized the most, then Thr$_9$, and then Thr$_{10}$ (Fig. 3 *B*). This trend was also observed in line-broadening of the Val (γH1, 5.20 Hz; γH2, 3.82 Hz), Thr$_9$ (γH, 3.18), and Thr$_{10}$ (γH, 2.95 Hz) γ protons (compare Fig. 1, *G* and *H*). These results indicate that the decapeptide residues outside the internalization motif have greater mobility than those within the motif. Therefore, the same residues known to be critical for internalization in vivo were immobilized in the presence of cages.

The internalization motif peptide could be interacting with multiple proteins in the lattice. To distinguish between the contributions of AP2 and clathrin, we prepared clathrin cages composed of either clathrin alone or clathrin plus purified AP2. AP2 alone could not be tested be-
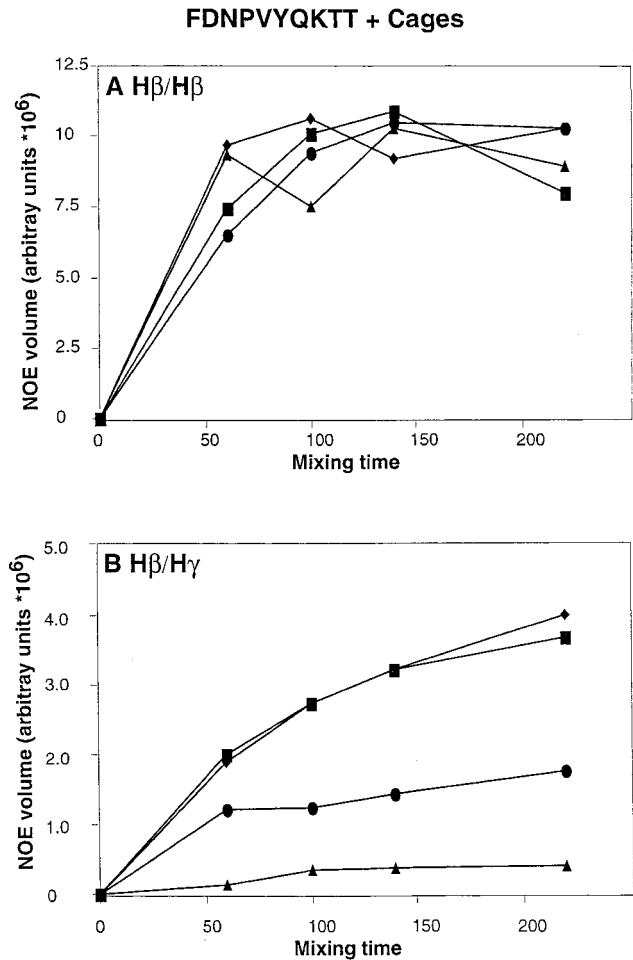

Figure 3. NOE buildup rates for fixed internuclear distances. NOE buildup curves from the sample containing the wild-type decapeptide with cages are shown for the intraresidue Hβ/Hβ NOEs of Phe (*squares*), Asn (*diamonds*), Pro (*circles*), and Tyr (*triangles*; *A*), and for the intraresidue Hβ/Hγ NOEs of Val(Hγ$_1$) (*squares*), Val(Hγ$_2$) (*diamonds*), Thr$_9$ (*circles*), and Thr$_{10}$ (*triangles*; *B*). Crosspeak intensities were calculated in arbitrary units of volume using the program Felix 2.30 from spectra acquired at 60, 100, 140, and 220 ms mixing times.

cause it aggregated under our experimental conditions. Fig. 4 shows that the wild-type hexapeptide in the presence of clathrin cages displayed distinct line-broadening (compare Fig. 4 *A* with Fig. 4 *B*). The mutant peptide, by contrast, showed much less line-broadening (compare Fig. 4 *D* with Fig. 4 *E*). Some additional line-broadening was seen when the wild-type peptide was mixed with cages composed of both clathrin and AP2 (compare Fig. 4 *B* with Fig. 4 *C*). However, it is likely that the broadening arose primarily from clathrin (see Discussion). The mutant peptide (Y$_{807}$S), by contrast, showed much less line-broadening (compare Fig. 4 *B* with Fig 4 *E*, and Fig. 4 *C* with Fig. 4 *F*). These results suggest that the LDL receptor interacts with clathrin through the FXNPXY motif during receptor clustering in coated pits.

We examined further the interaction between the hexapeptides and clathrin using recombinant portions of the clathrin molecule. The terminal domain of clathrin (resi-
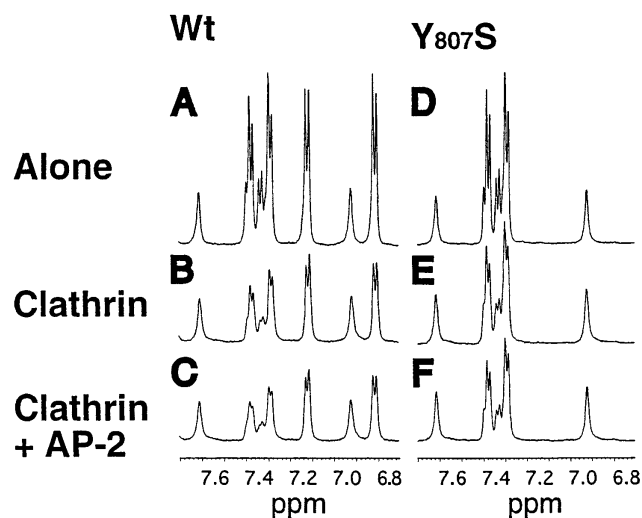
Figure 4. Differential broadening of the wild-type and mutant hexapeptides in the presence of assembled clathrin cages reconstituted with and without AP-2. Corresponding regions of 1-dimensional ^{1}H NMR from the aromatic region of the spectra are shown at absolute intensity. The indicated peptide (final concentration 1.5 mM) was added to buffer alone or buffer plus 9.7 mg/ml protein: FDNPVY alone (*A*), plus clathrin cages (*B*), plus clathrin and AP-2 cages (*C*), FDNPVS alone (*D*), plus clathrin cages (*E*), or plus clathrin and AP-2 cages. NMR samples were prepared as described for Fig. 1. Because of differing concentrations of peptide and protein, the absolute signal intensity can not be directly compared with those in Fig. 1.

Figure 5. Differential line-broadening of internalization peptides in the presence and absence of recombinant clathrin terminal domains and hubs. Corresponding regions of 1-dimensional ^{1}H NMR from the aromatic region of the spectra are shown at absolute intensity. Samples contained 1.0 mM peptide with or without 175 μM clathrin terminal domain TD(1–579) at pH 6.2 as follows: FDNPVY alone (*A*), plus TD(1–579) (*B*) or FDNPVS alone (*C*), plus TD(1–579) (*D*). The interactions of the wild-type hexapeptide (1 mM) with 200 μM of either TD(1–579) or clathrin Hub(1074–1483) were compared at pH 7.2 in 150 mM KCl. Samples contained: FDNPVY alone (*E*), plus TD(1–579) (*F*), or plus Hub(1074–1483) (*G*).

dues 1–579) expressed as a GST fusion protein was purified, and thrombin was cleaved from GST. Clathrin hubs (residues 1074–1483) were expressed as a hexaHis-tagged polypeptide, and were purified by a Ni resin and anion exchange. Line-broadening measurements were first made using the terminal domain at the acidic pH used in the cage assays. The wild-type peptide (Fig. 5) displayed the same degree of line-broadening (compare Fig. 5 *A* with Fig. 5 *B*) seen when peptide is incubated in the presence of clathrin cages. The mutant peptide, by contrast, displayed much less broadening (compare Fig. 5 *C* with Fig. 5 *D*). Equimolar amounts of either BSA or GST under the same conditions had no effect (data not shown). We saw a similar degree of line-broadening at neutral pH (compare Fig. 5 *E* with Fig. 5 *F*), but no appreciable broadening was detected when the hub region was substituted for the terminal domain at neutral pH (compare Fig. 5 *E* with Fig. 5 *G*). These results show that the LDL receptor tail selectively interacts with the terminal domain of clathrin.

The amino acid requirements at position 807 for LDL receptor internalization (14) have been found to correlate with the propensity of peptides from that region to form a reverse turn (2). We examined position 807 mutants for their ability to interact with clathrin terminal domains by measuring the change in peak intensity of 1D proton resonances for each peptide. Because peak heights are inversely proportional to the effective molecular weight, they can be used to calculate the relative binding constant for each peptide as it interacts with the terminal domain (see Materials and Methods). Table I shows that the rela-
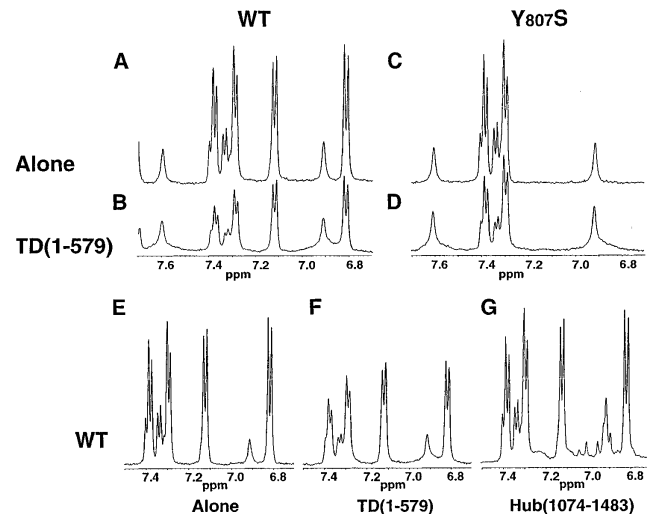
tive affinity of each peptide for the clathrin terminal domain strongly correlated with the predicted turn propensity (2) as well as the ability of receptors bearing these mutations to internalize LDL (14). Thus, peptides with Tyr and Phe at position 807 had the highest affinity, the greatest turn propensity, and the highest internalization rate, while a Leu at this position had an intermediate affinity and both Ser and Ala had the lowest affinities.

Transferred NOEs have been used previously to determine the conformation of peptides bound to proteins (26, 27, 49). These results have later been confirmed from crystal structures of the complexes (40, 57, 62). We used data from transferred NOE spectra to determine the structure of the FDNPVY motif bound to clathrin cages. Similar NOE results were obtained when cages were replaced with recombinant terminal domains (data not shown). Structures were calculated by simulated annealing (37) using 30 nontrivial transferred NOE restraints. Among these, 23 NOEs correspond to the residues NPVY, including the strong NH/NH NOE between Val and Tyr characteristic of a turn conformation (Fig. 6 *A*), and other short and intermediate range, structurally diagnostic NOEs. A superposition of the peptide backbones for the 21 structures with distance violations of <0.1 Å obtained among 30 calculated structures is shown in Fig. 6 *B*. All resulting structures had an extended NH$_2$ terminus followed by a Type 1 β turn around residues NPVY. The two NH$_2$-terminal amino acids did not align as well in the superposition. This result is more likely to arise from a lack of proton density in the extended structure of this region than

Peptide	K_d*	Internalization index‡	Turn propensity§
	mM		
FDNPVY	0.14	1.0	1.0
FDNPVF	0.33	0.95	0.75
FDNPVL	0.63	0.30	ND
FDNPVS	1.4	0.20	0
FDNPVA	3.1	0.20	0

*The relative K_d calculated from Phe(3,5) aromatic proton peak intensities as described in the experimental procedures. ‡Normalized to the native receptor (14). §Using NOE magnitudes as an indicator for turn propensity, scaled to that for the NPVY peptide (2). ND, not determined.

from increased mobility, since line-broadening and transferred NOE build-up rates indicate that Phe is immobilized (see above). The 21 calculated structures had a backbone root mean square deviation of 0.61 Å, indicating that a single conformational form of the peptide was bound by the cages. Based on this information, a representative structure is shown in Fig. 6 *C.*

Discussion

The surprising conclusion of this study is that clathrin may be the molecule in coated pits responsible for capturing the LDL receptor during receptor-mediated endocytosis. Four stringent criteria were used to distinguish specific from nonspecific interactions between the clustering motif peptide and clathrin. First, changing tyrosine 807 to serine, which matches the mutation that prevents LDL receptor clustering in coated pits (13), substantially reduced interaction of the peptide with the cages. Second, the wild-type peptide bound to the cages in a single conformation, and had the predicted (2, 12) reverse turn conformation. Third,
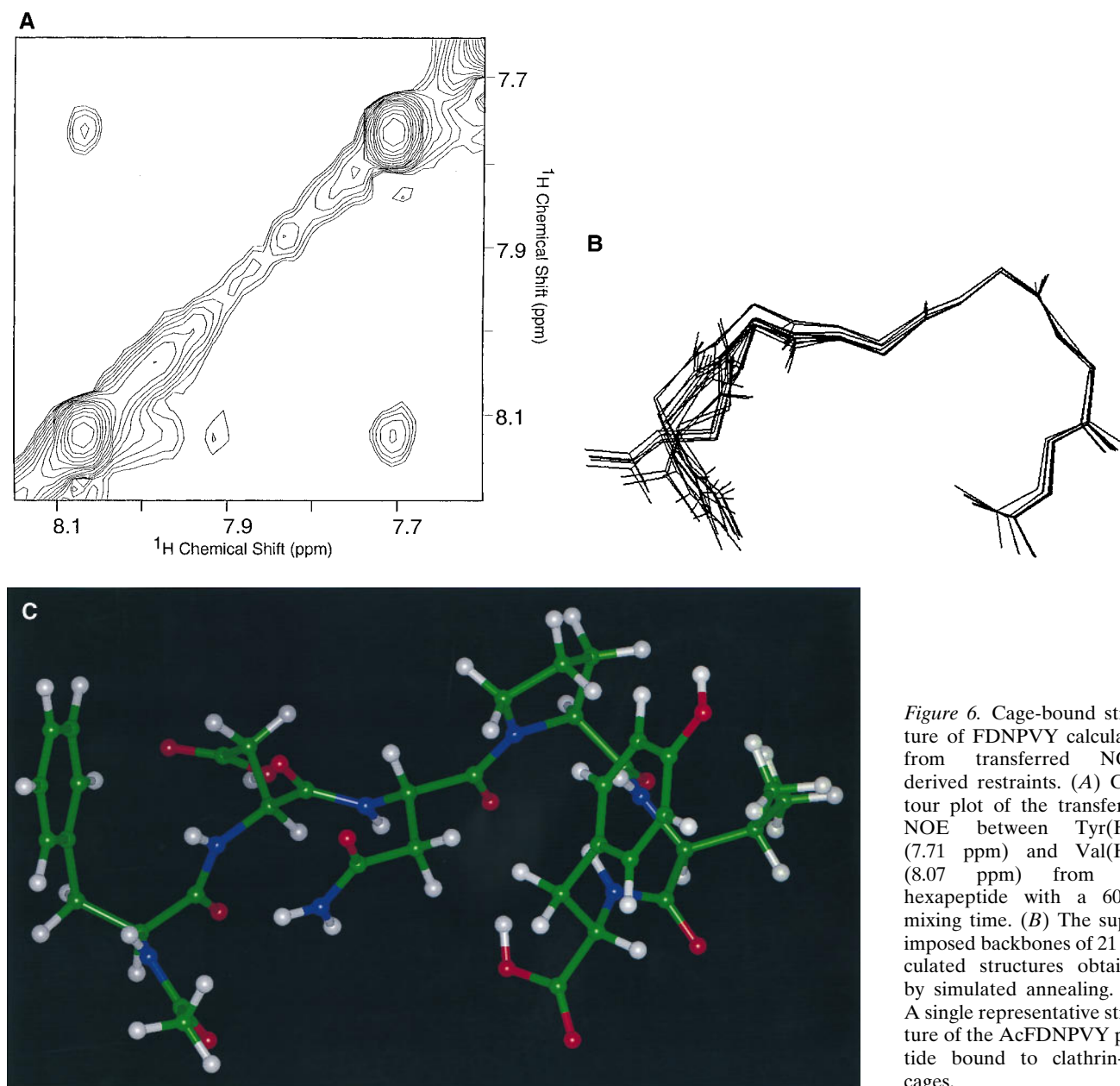

Figure 6. Cage-bound structure of FDNPVY calculated from transferred NOE-derived restraints. (*A*) Contour plot of the transferred NOE between Tyr(HN) (7.71 ppm) and Val(HN) (8.07 ppm) from the hexapeptide with a 60-ms mixing time. (*B*) The superimposed backbones of 21 calculated structures obtained by simulated annealing. (*C*) A single representative structure of the AcFDNPVY peptide bound to clathrin-AP cages.

binding was limited to those residues that lie within the FXNPXY motif. Fourth, once clathrin was identified as a candidate molecule, the wild-type peptide was found to interact with the terminal domain, but not with the hub portion of recombinant clathrin. Furthermore, the relative affinity of terminal domains for peptides with various position 807 substitutions correlated strongly with both the LDL receptor internalization index (14) and the predicted turn propensity (2). These results suggest that the receptor internalization rates depend on the affinities of the hexapeptide motif for clathrin, and that the affinity depends on a reverse turn conformation.

The apparent affinity we measured between the hexapeptides and clathrin terminal domains is in the same range as that reported for the interaction between YXXΦ peptides and the μ subunit of AP (4, 44). It is hard to judge the functional significance of these affinities. Within the cell, LDL receptors probably exist as multimers interacting with the rigid clathrin lattice in a two-dimensional plane (52). In this environment, the receptors will have a restricted rotational and translational mobility as they interact with a multivalent, nearly crystalline set of terminal domains. Assuming that a 76-nm–diameter clathrin-coated vesicle contains 60 clathrin triskelions (21), we calculated the concentration of terminal domains to be at minimum 1.5 mM. This result suggests the effective concentration of terminal domains in the region where receptor cluster is quite high, so the relatively low-affinity interactions we have measured should be sufficient to mediate clustering.

Clathrin terminal domains have been implicated before in receptor clustering (17, 18). The binding of β-arrestin to the phosphorylated cytoplasmic tail of the β₂-adrenergic receptor appears to be required for receptor migration to coated pits. The binding of β-arrestins to clathrin is stoichiometric, clustering in coated pits is coincident with receptor internalization, and expression of β-arrestin mediates internalization (18). The β-arrestin binding site has been localized to the first 100 amino acids of the clathrin heavy chain (17). Structural studies show that the terminal domain of clathrin is optimally positioned in an assembled lattice to interact with the cytoplasmic tails of receptors (53). However, none of these studies have sufficient resolution to determine the location of the terminal domains in an assembled clathrin coat.

Although clathrin terminal domains clearly interact with the NPXY clustering motif, we have not ruled out the possibility that APs can bind to the cytoplasmic portion of the LDL receptor, or that they can modulate the interaction of the NXPY motif with clathrin. The presence of AP2 in our clathrin cage preparations moderately enhanced line-broadening of the NMR spectra compared with clathrin alone, suggesting that the wild-type peptides may have a higher affinity for cages containing AP2 (Fig. 4). The bound peptide displayed a well-defined conformation in the presence or absence of APs, so broadening must be due to a single type of binding site for the hexapeptide. Therefore, most likely the enhanced broadening is not due to introduction of additional hexapeptide binding sites present in the APs.

Our results stand in contrast to previous studies showing that purified AP2 binds substoichiometrically to a fusion protein containing the cytoplasmic tail of the LDL receptor (42). The fusion protein used in this study contained 31 residues from the λcII protein, a thrombin cleavage site, 112 residues of myosin light chain, a second thrombin cleavage site, and the 50-residue LDL receptor tail (42). Interestingly, the cII fragment contains a dileucine motif that can directly interact with APs (20, 43). Since a fusion protein containing an internalization-defective LDL receptor tail (e.g., Y807C) was not tested, these studies did not rule out the possibility that the interaction with AP2 was mediated by the dileucine motif. Moreover, there is compelling in vivo evidence that AP2 does not cluster LDL receptors. Depletion of intracellular K⁺ and hypertonic treatment of cells both cause reversible loss of clathrin lattices from the cell surface (22, 28), which is accompanied by LDL receptor unclustering (22, 28). By contrast, these conditions do not uncluster AP2 (19). If receptor clustering were primarily dependent on AP2, then LDL receptors should have remained clustered under these conditions.

An important prediction from these results is that LDL receptors should be sorted and concentrated during clathrin-coated vesicle formation regardless of whether budding occurs from Golgi, endosome, or surface membranes. Coated vesicles purified from adrenal glands are enriched in masked LDL receptors four to fivefold (33). These isolated vesicles contain coated vesicle derived from both the plasma membrane and the Golgi apparatus that can be separated on the basis of size (5). Ligand blotting indicates that both populations of vesicles are equally enriched in LDL receptors relative to the plasma membrane (5). Therefore, even though there are no quantitative EM studies showing LDL receptors concentrated in Golgi-coated vesicles, these biochemical experiments suggest that sorting does occur.

AP2 does appear to be responsible for capturing receptors that contain YXXΦ (39) and dileucine internalization motifs (20, 43). Two-hybrid screen (38, 39) and surface plasmon resonance analysis (4, 39) both show that YXXΦ interacts with the μ chain of AP2. The properties of YXXΦ motif are distinct from those for FXNPXY since FXNPXY motifs did not bind the μ subunit, and a combinatorial library showed no preference for this motif (4). Dileucine motifs also bind clathrin AP2 and AP1, yet receptors with this motif do not compete with receptors containing YXXΦ during internalization (31). Receptor internalization by coated pits can therefore be mediated by at least three distinct motifs (two tyrosine-based and one dileucine-based), each of which is captured by a different binding site in the lattice.

Tyrosine phosphorylation alters the binding specificity of both YXXΦ and NPXY, although phosphorylation is not essential for binding to all phosphotyrosine binding (PTB) domains (6, 59). pYXXΦ binds SH₂ domains (46) while NPXpY binds proteins that contain a PTB domain (51). The structures of both pYXXΦ/SH₂ (16, 54, 55) and NPXpY/PTB domain (15, 60, 61) complexes have been solved. The former shows that pYXXΦ binds as an extended two-pronged plug. The structure of the latter confirms transferred NOE data (61) showing that the tyrosine in the bound NPXpY is in a tight turn preceded by an extended region. Since we found that bound FXNPXY is in a tight turn (Fig. 6 C), it is possible the simple addition of

phosphate or specific expression of a PTB domain blocks coated pit clustering. The conformation of YXXΦ bound to the μ chain of AP has not been determined, but if the phosphate is also what changes binding specificity, then the bound conformation of YXXΦ should be an extended, two-pronged plug rather than a tight turn.

This study demonstrates the power of NMR spectroscopy to identify the molecules in coat protein complexes responsible for sorting membrane proteins during vesicular traffic. At the same time, this method provides dynamic structural information about the targeting sequence when it is bound. Multiple targeting motifs regulate receptor trafficking throughout the cell. Internalization motifs can function at multiple steps along an internalization pathway, differentially using clathrin and AP subunits to generate different migratory patterns. The specificity of clathrin for FXNPXY and APs for YXXΦ appears to be as distinct as PTB and SH2 domains are for their phosphorylated counterparts. YXXΦ and dileucine motifs may target receptors to plasma membrane, late endosome, lysosome, and TGN structures via combinatorial interactions with AP complexes and possibly other membrane coats. By contrast, the FXNPXY motif may be needed for efficient clathrin-mediated recycling of LDL receptors between the plasma membrane and endosomes. Based only on the primary sequence of these motifs, it has not been possible to predict the cellular distribution of receptors. NMR spectroscopy should be useful to characterize further the conformational determinants of sorting motifs that ultimately determine receptor sorting patterns.

References

1. Anderson, R.G.W., J.L. Goldstein, and M.S. Brown. 1976. A mutation that impairs the ability of lipoprotein receptors to localize in coated pits on the cell surface of human fibroblasts. *Nature*. 270:695–699.
2. Bansal, A., and L.M. Gierasch. 1991. The NPXY internalization signal of the LDL receptor adopts a reverse-turn conformation. *Cell*. 67:1195–1201.
3. Bax, A., and S. Grzesiek. 1993. Methodological advances in protein NMR. *Acc. Chem. Res.* 26:132–138.
4. Boll, W., H. Ohno, Z. Songyang, I. Rapoport, L.C. Cantley, J.S. Bonifacino, and T. Kirchhausen. 1996. Sequence requirements for the recognition of tyrosine-based endocytic signals by clathrin AP-2 complexes. *EMBO (Eur. Mol. Biol. Organ.) J.* 15:5789–5795.
5. Bomsel, M., C. de Paillerets, H. Weintraub, and A. Alfsen. 1986. Lipid bilayer dynamics in plasma and coated vesicle membranes from bovine adrenal cortex. Evidence of two types of coated vesicle involved in the LDL receptor traffic. *Biochim. Biophys. Acta*. 859:15–25.
6. Borg, J.P., J. Ooi, E. Levy, and B. Margolis. 1996. The phosphotyrosine interaction domains of X11 and FE65 bind to distinct sites on the YENPTY motif of amyloid precursor protein. *Mol. Cell Biol.* 16:6229–6241.
7. Brewer, C.B., and M.G. Roth. 1991. A single amino acid change in the cytoplasmic domain alters the polarized delivery of influenza virus hemagglutinin. *J. Cell Biol.* 114:413–421.
8. Campbell, C., J. Squicciarini, M. Shia, P.F. Pilch, and R.E. Fine. 1984. Identification of a protein kinase as an intrinsic component of rat liver coated vesicles. *Biochemistry*. 23:4420–4426.
9. Chen, W.-J., J. Goldstein, and M.S. Brown. 1990. NPXY, a sequence often found in cytoplasmic tails, is required for coated pit-mediated internaliza-

tion of the low density lipoprotein receptor. *J. Biol. Chem*. 265:3116–3123.
10. Clore, G.M., and A.M. Gronenborn. 1982. Theory and applications of the transferred nuclear overhauser effect to the study of the conformations of small ligands bound to proteins. *J. Magn. Reson*. 48:402–417.
11. Clore, G.M., and A.M. Gronenborn. 1983. Theory of the time-dependent transferred nuclear overhauser effect: applications to structural analysis of ligand-protein complexes in solution. *J. Magn. Reson*. 53:423–442.
12. Collawn, J.F., M. Stangel, L.A. Kuhn, V. Esekogwu, S. Jing, I.S. Trowbridge, and J.A. Tainer. 1990. Transferrin receptor internalization sequence YXRF implicates a tight turn as the structural recognition motif for endocytosis. *Cell*. 63:1061–1072.
13. Davis, C.G., M.A. Lehrman, D.W. Russell, R.G. Anderson, M.S. Brown, and J.L. Goldstein. 1986. The J.D. mutation in familial hypercholesterolemia: amino acid substitution in cytoplasmic domain impedes internalization of LDL receptors. *Cell*. 45:15–24.
14. Davis, C.G., I.R. van Driel, D.W. Russell, M.S. Brown, and J.L. Goldstein. 1987. The low density lipoprotein receptor. Identification of amino acids in cytoplasmic domain required for rapid endocytosis. *J. Biol. Chem*. 262:4075–4082.
15. Eck, M.J., S. Dhe-Paganon, T. Trub, R.T. Nolte, and S.E. Shoelson. 1996. Structure of the IRS-1 PTB domain bound to the juxtamembrane region of the insulin receptor. *Cell*. 85:695–705.
16. Eck, M.J., S.E. Shoelson, and S.C. Harrison. 1993. Recognition of a high-affinity phosphotyrosyl peptide by the Src homology-2 domain of p56lck. *Nature*. 362:87–91.
17. Goodman, O.B., Jr., J.G. Krupnick, V.V. Gurevich, J.L. Benovic, and J.H. Keen. 1997. Arrestin/clathrin interaction. Localization of the arrestin binding locus to the clathrin terminal domain. *J. Biol. Chem*. 272:15017–15022.
18. Goodman, O.B., Jr., J.G. Krupnick, F. Santini, V.V. Gurevich, R.B. Penn, A.W. Gagnon, J.H. Keen, and J.L. Benovic. 1996. Beta-arrestin acts as a clathrin adaptor in endocytosis of the beta2-adrenergic receptor. *Nature*. 383:447–450.
19. Hansen, S.H., K. Sandvig, and B. van Deurs. 1993. Clathrin and HA2 adaptors: effects of potassium depletion, hypertonic medium, and cytosol acidification. *J. Cell Biol*. 121:61–72.
20. Heilker, R., U. Manning-Krieg, J.F. Zuber, and M. Spiess. 1996. In vitro binding of clathrin adaptors to sorting signals correlates with endocytosis and basolateral sorting. *EMBO (Eur. Mol. Biol. Organ.) J*. 15:2893–2899.
21. Heuser, J., and T. Kirchhausen. 1985. Deep-etch views of clathrin assemblies. *J. Ultrastruct. Res*. 92:1–27.
22. Heuser, J.E., and R.G. Anderson. 1989. Hypertonic media inhibit receptor-mediated endocytosis by blocking clathrin-coated pit formation. *J. Cell Biol*. 108:389–400.
23. Keen, J.H. 1990. Clathrin and associated assembly and disassembly proteins. *Annu. Rev. Biochem*. 59:415–438.
24. Keen, J.H., K.A. Beck, T. Kirchhausen, and T. Jarrett. 1991. Clathrin domains involved in recognition by assembly protein AP-2. *J. Biol. Chem*. 266:7950–7956.
25. Keen, J.H., M.C. Willingham, and I.H. Pastan. 1979. Clathrin-coated vesicles: isolation, dissociation and factor-dependent reassociation of clathrin baskets. *Cell*. 16:303–312.
26. Landry, S.J., R. Jordan, R. McMacken, and L.M. Gierasch. 1992. Different conformations for the same polypeptide bound to chaperones DnaK and GroEL. *Nature*. 355:455–457.
27. Landry, S.J., A. Taher, C. Georgopoulos, and S.M. van der Vies. 1996. Interplay of structure and disorder in cochaperonin mobile loops. *Proc. Natl. Acad. Sci. USA*. 93:11622–11627.
28. Larkin, J.M., W.C. Donzell, and R.G. Anderson. 1986. Potassium-dependent assembly of coated pits: new coated pits form as planar clathrin lattices. *J. Cell Biol*. 103:2619–2627.
29. Liu, S.H., M.L. Wong, C.S. Craik, and F.M. Brodsky. 1995. Regulation of clathrin assembly and trimerization defined using recombinant triskelion hubs. *Cell*. 83:257–267.
30. Mahaffey, D.T., J.S. Peeler, F.M. Brodsky, and R.G. Anderson. 1990. Clathrin-coated pits contain an integral membrane protein that binds the AP-2 subunit with high affinity. *J. Biol. Chem*. 265:16514–16520.
31. Marks, M.S., L. Woodruff, H. Ohno, and J.S. Bonifacino. 1996. Protein targeting by tyrosine- and di-leucine-based signals: evidence for distinct saturable components. *J. Cell Biol*. 135:341–354.
32. Matter, K., J.A. Whitney, E.M. Yamamoto, and I. Mellman. 1993. Common signals control low density lipoprotein receptor sorting in endosomes and the Golgi complex of MDCK cells. *Cell*. 74:1053–1064.
33. Mello, R.J., M.S. Brown, J.L. Goldstein, and R.G. Anderson. 1980. LDL receptors in coated vesicles isolated from bovine adrenal cortex: binding sites unmasked by detergent treatment. *Cell*. 20:829–837.
34. Murphy, J.E., and J.H. Keen. 1992. Recognition sites for clathrin-associated proteins AP-2 and AP-3 on clathrin triskelia. *J. Biol. Chem*. 267:10850–10855.
35. Nesterov, A., H.S. Wiley, and G.N. Gill. 1995. Ligand-induced endocytosis of epidermal growth factor receptors that are defective in binding adaptor proteins. *Proc. Natl. Acad. Sci. USA*. 92:8719–8723.
36. Ni, F., Y. Konishi, R.B. Frazier, H.A. Scheraga, and S.T. Lord. 1989. High-

resolution NMR studies of fibrinogen-like peptides in solution: interaction of thrombin with residues 1–23 of the A alpha chain of human fibrinogen. *Biochemistry*. 28:3082–3094.

37. Nilges, M., G.M. Clore, and A.M. Gronenborn. 1988. Determination of three-dimensional structures of proteins from interproton distance data by dynamical simulated annealing from a random array of atoms. Circumventing problems associated with folding. *FEBS Lett*. 239:129–136.

38. Ohno, H., M.C. Fournier, G. Poy, and J.S. Bonifacino. 1996. Structural determinants of interaction of tyrosine-based sorting signals with the adaptor medium chains. *J. Biol. Chem*. 271:29009–29015.

39. Ohno, H., J. Stewart, M.C. Fournier, H. Bosshart, I. Rhee, S. Miyatake, T. Saito, A. Gallusser, T. Kirchhausen, and J.S. Bonifacino. 1995. Interaction of tyrosine-based sorting signals with clathrin-associated proteins. *Science*. 269:1872–1875.

40. Park, H.W., S.R. Boduluri, J.F. Moomaw, P.J. Casey, and L.S. Beese. 1997. Crystal structure of protein farnesyltransferase at 2.25 angstrom resolution. *Science*. 275:1800–1804.

41. Pearse, B.M., and M.S. Robinson. 1990. Clathrin, adaptors, and sorting. *Annu. Rev. Cell Biol*. 6:151–171.

42. Pearse, B.M.F. 1988. Receptors compete for adaptors found in plasma membrane coated pits. EMBO (*Eur. Mol. Biol. Organ.*) *J*. 7:3331–3336.

43. Rapoport, I., Y.C. Chen, P. Cupers, S.E. Shoelson, and T. Kirchhausen. 1998. Dileucine-based sorting signals bind to the beta chain of AP-1 at a site distinct and regulated differently from the tyrosine-based motif-binding site. *EMBO (Eur. Mol. Biol. Organ.) J*. 17:2148–2155.

44. Rapoport, I., M. Miyazaki, W. Boll, B. Duckworth, L.C. Cantley, S. Shoelson, and T. Kirchhausen. 1997. Regulatory interactions in the recognition of endocytic sorting signals by AP-2 complexes. *EMBO (Eur. Mol. Biol. Organ.) J*. 16:2240–2250.

45. Rohrer, J., A. Schweizer, D. Russell, and S. Kornfeld. 1996. The targeting of Lamp1 to lysosomes is dependent on the spacing of its cytoplasmic tail tyrosine sorting motif relative to the membrane. *J. Cell Biol*. 132:565–576.

46. Songyang, Z., S.E. Shoelson, M. Chaudhuri, G. Gish, T. Pawson, W.G. Haser, F. King, T. Roberts, S. Ratnofsky, R.J. Lechleider, et al. 1993. SH2 domains recognize specific phosphopeptide sequences. *Cell*. 72:767–778.

47. Sorkin, A., and G. Carpenter. 1993. Interaction of activated EGF receptors with coated pit adaptins. *Science*. 261:612–615.

48. States, D.J., R.A. Haberkorn, and D.J. Ruben. 1982. A two-dimensional nuclear overhauser experiment with pure absorption phase in four quadrants. *J. Magn. Reson*. 48:286–292.

49. Stradley, S.J., J. Rizo, and L.M. Gierasch. 1993. Conformation of a heptapeptide substrate bound to protein farnesyltransferase. *Biochemistry*. 32:12586–12590.

50. Trowbridge, I.S., J.F. Collawn, and C.R. Hopkins. 1993. Signal-dependent membrane protein trafficking in the endocytic pathway. *Annu. Rev. Cell Biol*. 9:129–161.

51. van der Geer, P., S. Wiley, G.D. Gish, V.K. Lai, R. Stephens, M.F. White, D. Kaplan, and T. Pawson. 1996. Identification of residues that control specific binding of the Shc phosphotyrosine-binding domain to phosphotyrosine sites. *Proc. Natl. Acad. Sci. USA*. 93:963–968.

52. van Driel, I.R., C.G. Davis, J.L. Goldstein, and M.S. Brown. 1987. Self-association of the low density lipoprotein receptor mediated by the cytoplasmic domain. *J. Biol. Chem*. 262:16127–16134.

53. Vigers, G.P., R.A. Crowther, and B.M. Pearse. 1986. Three-dimensional structure of clathrin cages in ice. *EMBO (Eur. Mol. Biol. Organ.) J*. 5:529–534.

54. Waksman, G., D. Kominos, S.C. Robertson, N. Pant, D. Baltimore, R.B. Birge, D. Cowburn, H. Hanafusa, B.J. Mayer, M. Overduin, et al. 1992. Crystal structure of the phosphotyrosine recognition domain SH2 of v-src complexed with tyrosine-phosphorylated peptides. *Nature*. 358:646–653.

55. Waksman, G., S.E. Shoelson, N. Pant, D. Cowburn, and J. Kuriyan. 1993. Binding of a high affinity phosphotyrosyl peptide to the Src SH2 domain: crystal structures of the complexed and peptide-free forms. *Cell*. 72:779–790.

56. Warren, R.A., F.A. Green, and C.A. Enns. 1997. Saturation of the endocytic pathway for the transferrin receptor does not affect the endocytosis of the epidermal growth factor receptor. *J Biol. Chem*. 272:2116–2121.

57. Xu, Z., A.L. Horwich, and P.B. Sigler. 1997. The crystal structure of the asymmetric GroEL-GroES-(ADP)$_7$ chaperonin complex. *Nature*. 288: 741–750.

58. Zhang, J.Z., B.A. Davletov, T.C. Südhof, and R.G.W. Anderson. 1994. Synaptotagmin is a high affinity receptor for clathrin AP-2: implications for membrane recycling. *Cell*. 78:751–760.

59. Zhang, Z., C.H. Lee, V. Mandiyan, J.P. Borg, B. Margolis, J. Schlessinger, and J. Kuriyan. 1997. Sequence-specific recognition of the internalization motif of the Alzheimer's amyloid precursor protein by the X11 PTB domain. *EMBO (Eur. Mol. Biol. Organ.) J*. 16:6141–6150.

60. Zhou, M.M., B. Huang, E.T. Olejniczak, R.P. Meadows, S.B. Shuker, M. Miyazaki, T. Trub, S.E. Shoelson, and S.W. Fesik. 1996. Structural basis for IL-4 receptor phosphopeptide recognition by the IRS-1 PTB domain. *Nat. Struct. Biol*. 3:388–393.

61. Zhou, M.M., K.S. Ravichandran, E.F. Olejniczak, A.M. Petros, R.P. Meadows, M. Sattler, J.E. Harlan, W.S. Wade, S.J. Burakoff, and S.W. Fesik. 1995. Structure and ligand recognition of the phosphotyrosine binding domain of Shc. *Nature*. 378:584–592.

62. Zhu, X., X. Zhao, W.F. Burkholder, A. Gragerov, C.M. Ogata, M.E. Gottesman, and W.A. Hendrickson. 1996. Structural analysis of substrate binding by the molecular chaperone DnaK. *Science*. 272:1606–1614.